## Title

LINAC INJECTION FOR THE 340-Mev BERKELEY ELECTRON SYNCHROTRON: PART II - EXPERIMENTAL

## Permalink

https://escholarship.org/uc/item/4rm219r6

## Authors

Crebbin, K.C.
Everette, W.L.

## Publication Date

1960-02-01

UCRL 9103

UNIVERSITY OF
CALIFORNIA
Ernest O. Lawrence
Radiation
Laboratory

# LINAC INJECTION FOR THE 340-MEV BERKELEY ELECTRON SYNCHROTRON
## PART II- EXPERIMENTAL

UCRL-9103
Particle Accelerators and
High-Voltage Machines
TID-4500 (15th Ed.)

UNIVERSITY OF CALIFORNIA

Lawrence Radiation Laboratory
Berkeley, California

Contract No. W-7405-eng-48

# LINAC INJECTION FOR THE 340-MEV BERKELEY ELECTRON SYNCHROTRON: PART II - EXPERIMENTAL

K. C. Crebbin and W. L. Everette

February 1960

Printed in USA. Price $.75 Available from the
Office of Technical Services
U. S. Department of Commerce
Washington 25, D. C.

# LINAC INJECTION FOR THE 340-MEV BERKELEY ELECTRON SYNCHROTRON: PART II - EXPERIMENTAL

K. C. Crebbin and W. L. Everette

Lawrence Radiation Laboratory
University of California
Berkeley, California

February 1960

## ABSTRACT

In this report we consider the problems of linac injection into the Berkeley synchrotron. We cover original inflector design and its modification, beam alignment, and preliminary results. Some indication is given of future tests that would have been made if the project had not been discontinued owing to the shutdown of the synchrotron. At the end of the testing, we had beam around one turn but were unable to get any indication of beam pickup and acceleration by the rf.

Theory and calculations relevant to linac injection are presented in Part I of this report: K. C. Crebbin and J. R. Hiskes, Linac Injection for the 340-Mev Berkeley Electron Synchrotron: Part I -- Theoretical, UCRL-9057, January 1960.

# LINAC INJECTION FOR THE 340-MEV BERKELEY ELECTRON SYNCHROTRON: PART II - EXPERIMENTAL

K. C. Crebbin and W. L. Everette

Lawrence Radiation Laboratory
University of California
Berkeley, California

February 1960

## I. INFLECTOR DESIGN AND VOLTAGE TESTING

Particles must be brought in tangent to an orbit to be injected into a magnetic field. A completely circular machine imposes a more difficult inflector-design problem than one with straight sections. Small physical size of the vacuum chamber creates additional difficulties.

A cross section of the Berkeley synchrotron vacuum chamber, pole tips, and pole-tip supporting rings is shown in Fig. 1. Figure 2 is a plan view of the vacuum chamber and pole-tip supporting rings. The vacuum chamber was modified as shown in Fig. 3 to permit tangential injection of electrons at a point on the north-south center line of the machine.

The original inflector is shown in Fig. 4. This failed to hold the necessary 70 kv. A modified design having the same electrical field shape is shown in Fig. 5. This design held the necessary voltage with sufficient margin of safety for reliable operation. However, it could not be moved far enough away from the center of the vacuum chamber to provide the necessary radial aperture for acceleration.* The section marked "A" in Fig. 3 limits the radial motion of this type of inflector.

To provide injection using the existing vacuum chamber required a complete redesign of the inflector. The tangent point of the beam to an orbit as it leaves the inflector was moved back into the "dog-leg" section as shown in Fig. 6. A desirable trajectory was selected starting at the same radial position as the present 100-kv electron gun. The path through the inflector was taken with a constant radius of curvature $\rho$. The necessary electric field to provide this $\rho$ in the magnetic field was then computed for positions 1-in. apart along the beam line. The beam trajectory of a particle coming through the fringe field was then computed. This was calculated along a line tangent to an orbit at the north-south center line of the manget. This tangent line was the reference line for all calculations and beam-alignment measurements. The point was found along this tangential line

---

* The orbit expands by a 2-cm radius during acceleration (i.e., from the injection energy of 2 Mev to peak synchrotron energy of 340 Mev). This is caused by the 2% change in electron velocity with no corresponding change in oscillator frequency.

at which the two trajectories have the same angle with respect to the line and the same tanjential position along the line. This was chosen as the other end of the inflector. The necessary offset to join the two trajectories was provided by a pair of steering electrodes. This pair of electrodes provided position and angular adjustment of the beam. These two adjustments are necessary if the beam is to be placed tangent to an orbit at the output end of the inflector. The trajectories with and without the steering electrodes are shown in Fig. 7. The trajectory calculations are given in the Appendix.

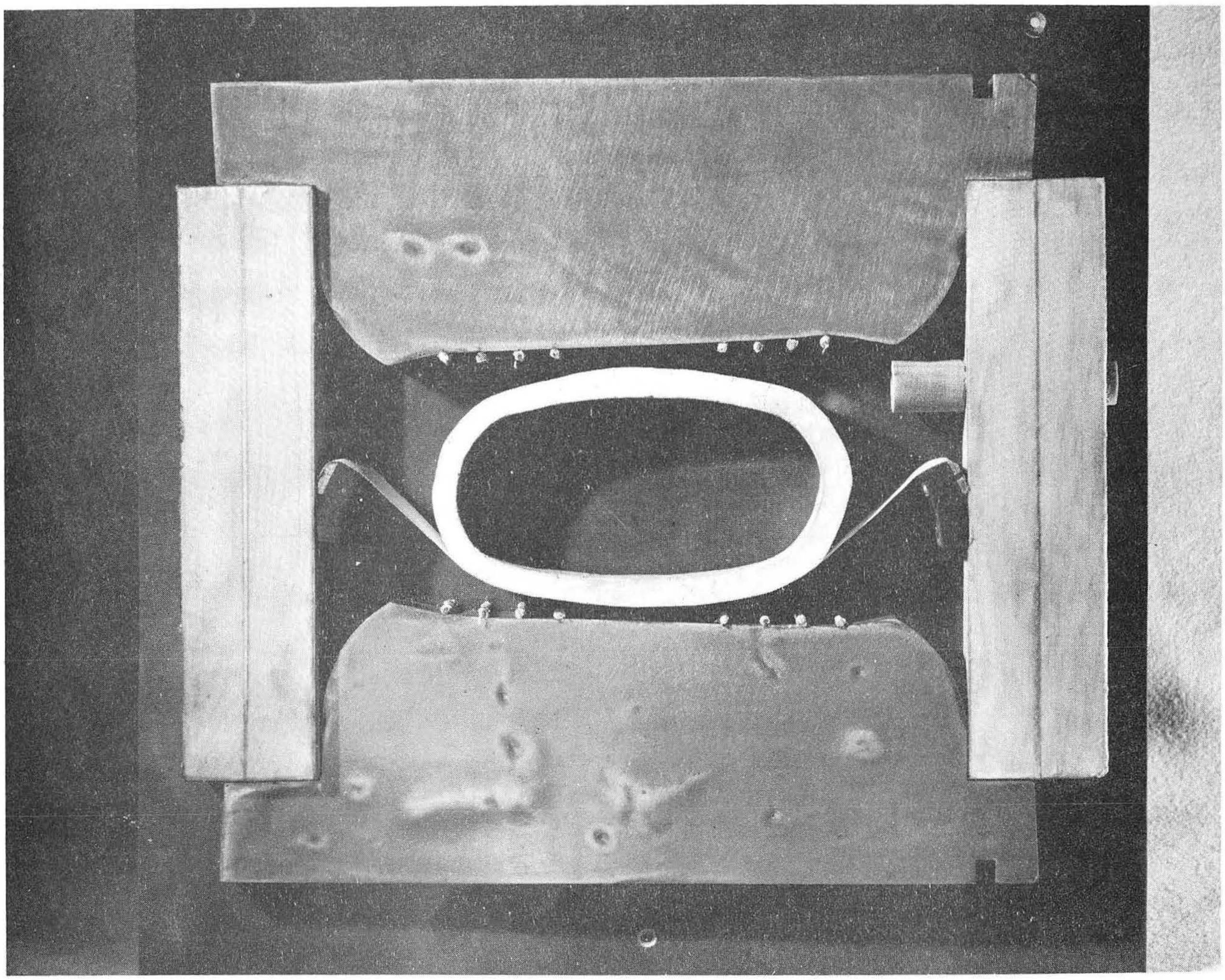

ZN-2374

Fig. 1. Cross section of pole tips and vacuum chamber.

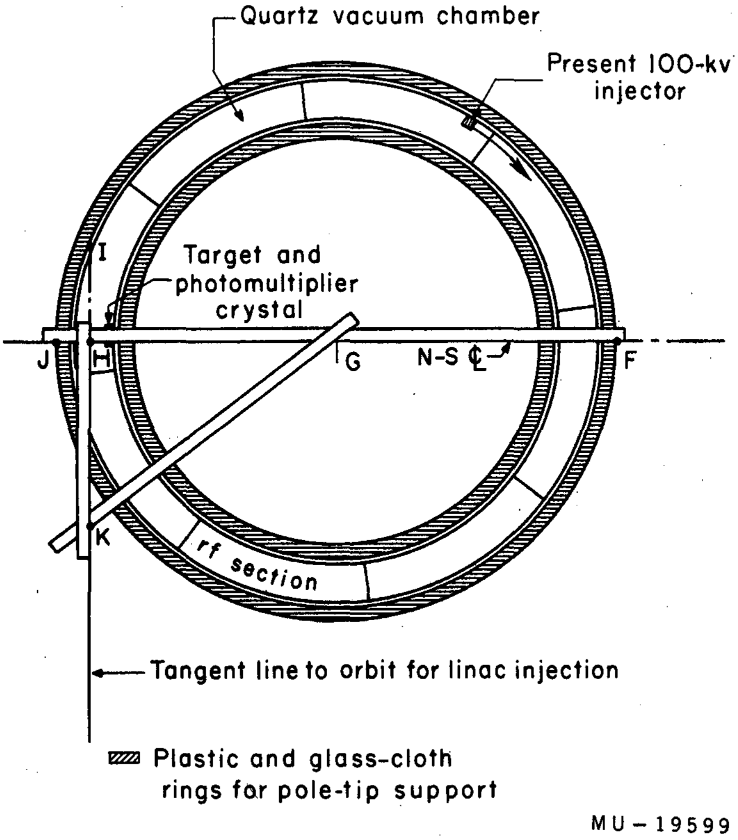

Fig. 2. Plan view of vacuum chamber and support rings. (Scale: 1/16.)

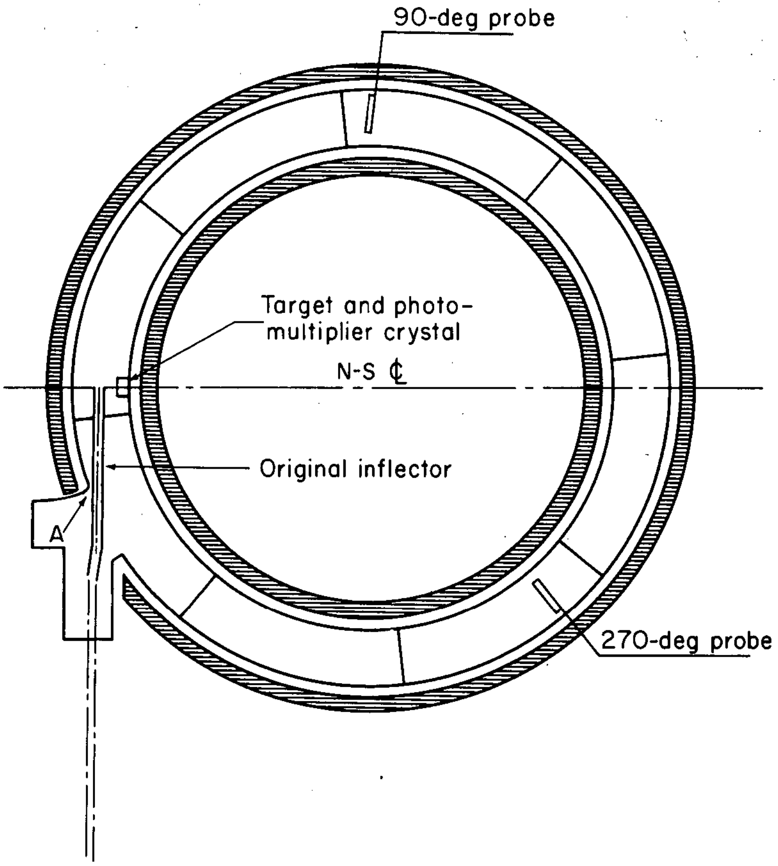

MU-19600

Fig. 3. Vacuum chamber modified for linac injection. (Not to scale.)

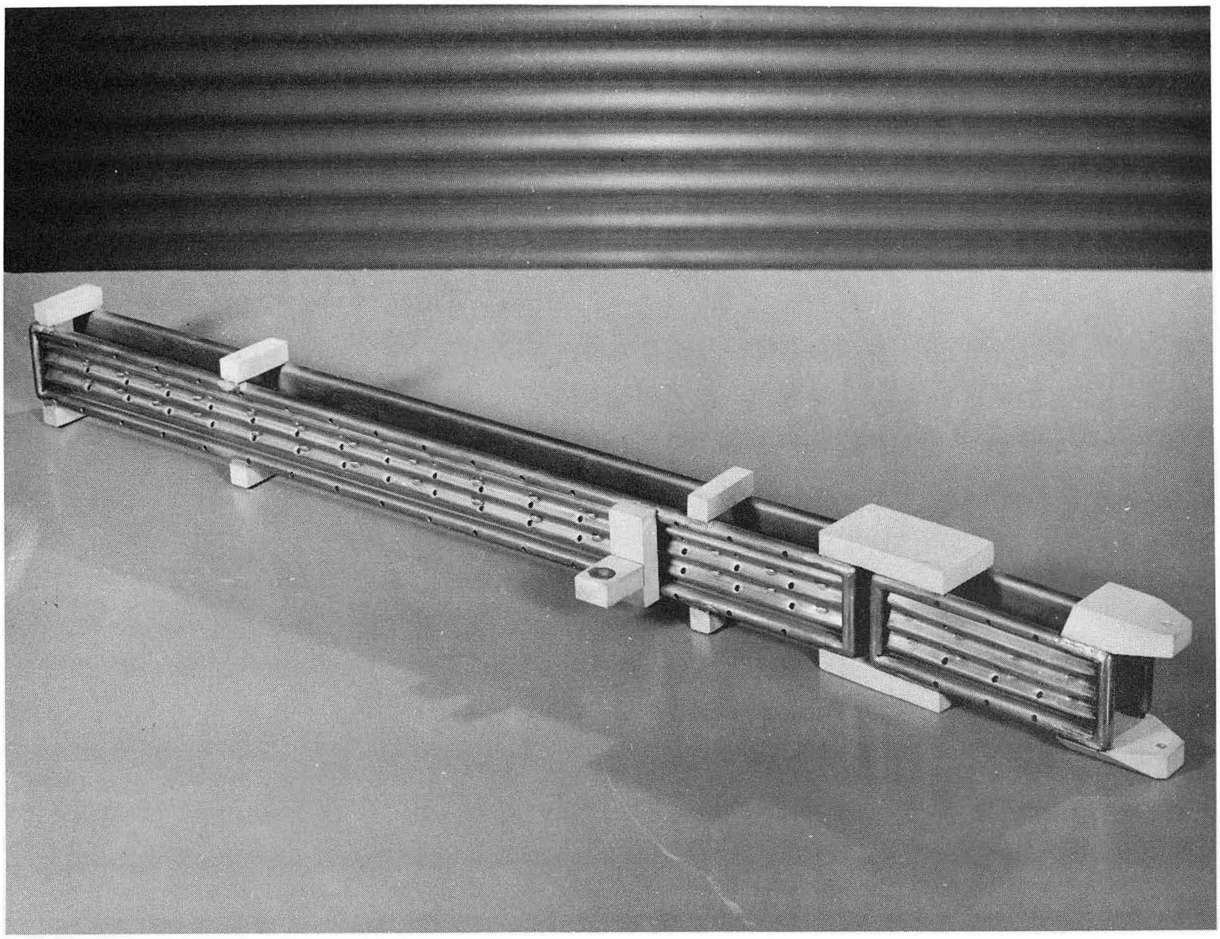

ZN-2375

Fig. 4. Original inflector.

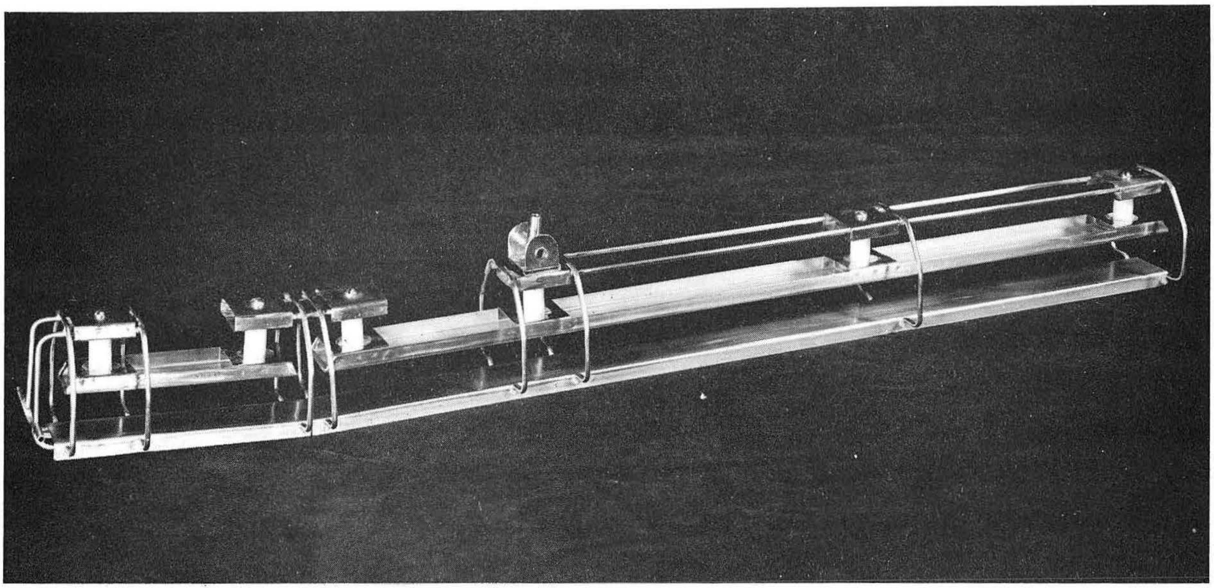

ZN-2376

Fig. 5. Modified inflector.

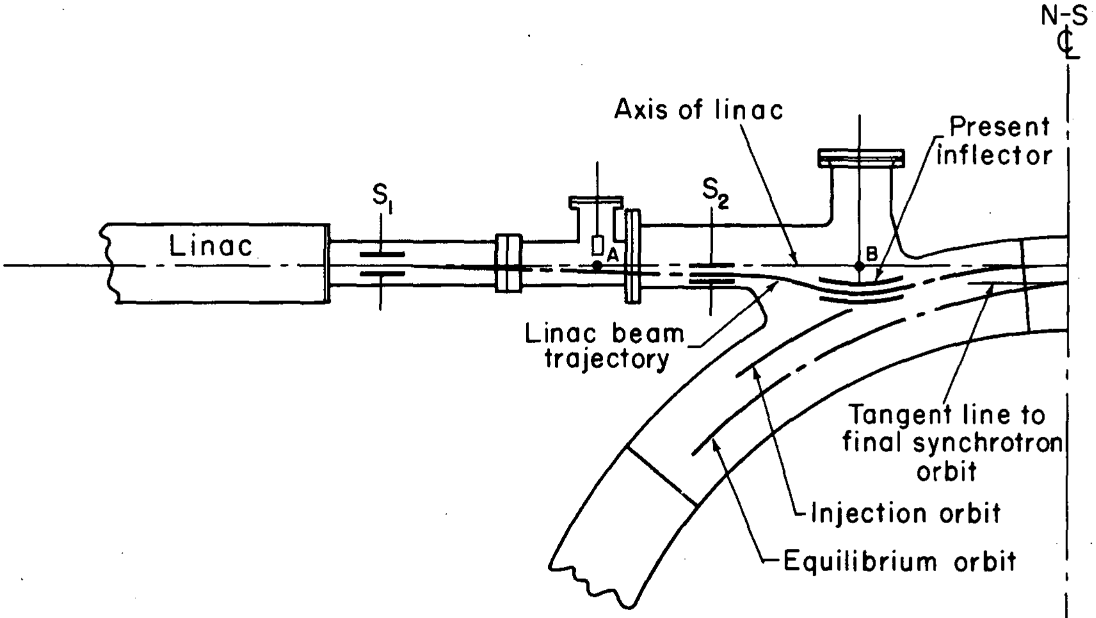

MU-19601

Fig. 6. Present inflector and beam-pipe geometry.
(Scale: 1/8.)

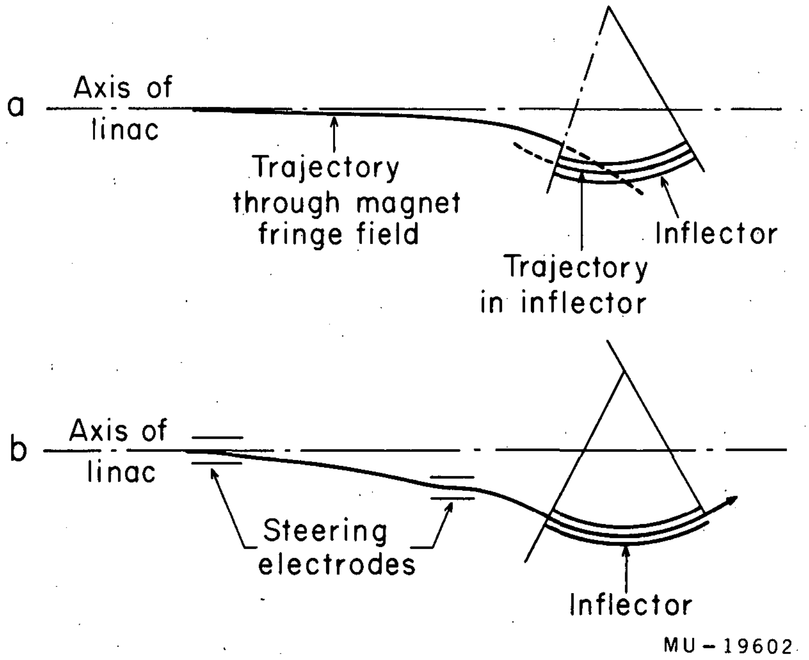

Fig. 7. (a) Injection trajectory without steering electrodes; (b) Injection trajectory with steering electrodes.

## II. LINEAR ACCELERATOR ALIGNMENT

Two methods were used in placing the linac waveguides in proper position for injection. A reference line-of-sight was established along the tangent line from point H, Fig. 2, and an optical alignment of the machine was made. The actual beam position was then determined by photographs, and necessary electrical corrections were made to guide the beam along the desired trajectory.

We were fortunate to have the linac ready for installation at a time when the synchrotron was dismantled for repairs. With the top portion of the magnet yoke and the upper pole tips removed, easy access to the orbital region was gained. We proceeded to locate the beam-orbit height. In a plan view of this region, Fig. 2 for example, the bare pole-tip support rings may be seen. The diameter and height variations of these rings are respectively ± 0.010 in. and 0.005 in. These rings hold the pole tips in position to permit a uniform gap around the orbit circle, and the focus field established by this geometry forces the beam to move in the median plane of this gap. We could then assume that this plane must also be the median plane of the support rings. Point I, Fig. 2, was marked on the ring wall at this height. Our assumption was later confirmed by a measurement of the height of ultraviolet radiation stains on the inner wall of the vacuum segments.

Locating the orbit was easy; constructing a tangent line of sight coplanar with the orbit was not. Two physical circumstances guided us in this task. The only accessible area in which to place the linac was at the northwest corner of the magnet. A north-south center-line index was already established on the support rings. This was an aid in locating the orbit center and setting up the tangent line. Also, the orbit plane was level to gravity, which made possible the alignment of the machine in this plane with a bubble level.

Let us refer to Fig. 2. The orbit circle was bisected by a straight-edged steel bar extending through points F and J. Point G was located on the bar as the orbit center, and the radius GH was laid out. Two additional steel bars were used to construct a right-angled triangle on top of the support rings. The side proportions of this triangle were 3, 4, and 5. The "3" side was extended parallel to the tangent line. Two thin-fiber plumb lines, dropped from points H and K, established the proper line of sight for north-south alignment. Alignment was then accomplished by sighting along the guide axis, keeping the exit aperture centered in the entrance hole. In the final position these apertures were brought into line with point I and the two plumb lines, keeping the waveguides level to gravity. Fine adjustments were made with the waveguide mounting-cradle-adjustment screws.

With the machine now in position, the linac beam was brought on and the actual trajectory was located. Two methods of "photographing" the beam were used. Exposure of glass plates to the beam causes absorption bands in the glass, and with a proper exposure, glass accurately records the cross-sectional appearance of the beam. Also, when a plate of Lucite is bombarded, local heating causes the Lucite to melt and reveals the beam size. Both methods may be used in air. Only glass should be used in vacuum because of excessive "outgassing" of the plastic.

Initial Lucite exposures at 4 in. beyond the accelerating waveguides showed the beam to be 3/16 in. low and 1/4 in to the south of the axis. This deflection was due to the earth's magnetic field. In view of transit time, the beam spends more time in the earth's field along the injector region than at any other point along its accelerating path. Consequently, a single correction at this end proved sufficient. An air-core coil capable of 1500 ampere-turns was placed near the injector-gun anode flange and oriented such that its field could compensate for the earth's field deflection. Proper compensation was determined by increasing the coil current until optimum response was obtained from a "bulls-eye" beam collector. This collector had a 1/8-in. aperture and was positioned on the optical axis. At maximum response the beam was within 1/32 in. from the axis at this point.

## III. INJECTION TESTS

A few weeks after the synchrotron was reassembled we tried the first linac injection. Operating conditions were re-established to bring the beam out of the linac along the optical axis, and the beam pipe was installed connecting the two vacuum systems. Figure 6 shows this setup. The distances from the two access-port flanges to the optical axis at points A and B were established, and glass-plate exposures were taken to locate the beam position. With the magnet field off, the beam was well on the axis at both points.

The maximum inflector voltage before excessive sparking commenced was about 62 kv. This voltage fixed the injection energy at 2 Mev and the injection time at roughly 115 μsec after the scope trigger. The intensity of the magnet at this time was not high enough to cause a perceptible change in the beam position at point A. Deflection from point B was 1-1/4 in., and since the axis of the inflector was to be 1-1/2 in. from the optical axis, the steering electrodes were needed for the additional 1/4 in. of orbit displacement.

The first steering electrode, $S_1$ in Fig. 6, was centered on the beam axis. The second, $S_2$, was offset 9/32 in., since the beam was already off by 5/32 in. at this point owing to the magnet field. A beam probe was used to locate the beam at the inflector input position. The collector plate was the same width as the electrode gap and was placed coincident with the input end. The electrode voltage was calculated and set for 1/4 in. displacement of the 2-Mev beam, and the linac beam energy was varied until a maximum response was obtained. We then varied the steering-electrode voltage to confirm the energy. The inflector was then substituted for the probe. A second probe was installed in the synchrotron target port to determine if the inflector did its job. A 2-Mev filter was placed ahead of this probe to shield it from scattered low-energy electrons. A peak pulse current of 3 ma was monitored from the probe for the 2-Mev operating conditions.

The target-port probe was withdrawn and the 90-deg probe (Fig. 2.) was installed. Slight corrections in timing and electrode voltages were required to guide the beam around to this point. One to 2 ma of current was monitored at the 90- and 270-deg probe position without further changes in operating conditions. A glass-plate beam exposure was made at the inside port just after the rf gap and just ahead of the inflector. This position was as near to a complete turn as we could track the beam. The exposure pattern at this point was cigar-shaped, 3/8-in. maximum vertical height and 1-1/2-in. in horizontal length, centered 5/8 in. interior to the vacuum-segment center line.

## IV. RF AND BOOSTER PICKUP ATTEMPTS

The beam from the 100-kev injector is accelerated to about 2 Mev by betatron action. The radio frequency (rf) is then turned on and accelerates the beam to 340 Mev. The flux bars that provide the betatron accelerating flux saturate too soon to permit turning on the rf at constant frequency. To overcome this, additional flux is provided for acceleration by two units called boosters. They dump a current through a coil around the flux bars. This additional "boost" gives the particles enough additional energy to permit turn-on of the rf at constant frequency.

The internal beam in the synchrotron is monitored by a crystal light pipe and photomultiplier tube mounted just past the target on the inside of the vacuum system. Any beam that spirals in strikes the target, and some scattered particles strike the photomultiplier crystal. The signal from this tube is observed on an oscilloscope.

Peaking strips in the magnetic field provide trigger signals to turn on all equipment associated with the acceleration. The first signal is used as a scope trigger. For the following discussion, zero time will be taken as the start of the scope pulse.

Normal 100-kev injection occurs at 7 μsec. The beam that falls in at the end of the betatron acceleration is called betatron beam. This is observed at 110 μsec without boosters, and at 160 μsec with boosters. The photomultiplier tube becomes inoperative at about 200 μsec owing to stray magnetic field. The linac-injected beam is observed at 115 μsec. This places it below the energy necessary for constant rf acceleration. Therefore, attempts were made to pick up the beam with the boosters and then the rf. The photomultiplier crystal is in direct line with the linac beam, as can be seen in Fig. 2. The high intensity of scattered beam and x-rays from the linac beam caused blocking of the photomultiplier circuit for about 80 μsec after the linac beam was turned off. This can be seen in Fig. 8. This made it impossible to see if any beam was carried around by the boosters a number of turns before spiraling into the target.

The external x-ray beam (340 Mev) is monitored by ionization chambers and a photomultiplier tube. The photomultiplier tube was moved to within 6 ft. of the target and the collimater removed. No trace of beam was observed.

Because of the shutdown of the synchrotron, linac-injection experiments were terminated at this point.

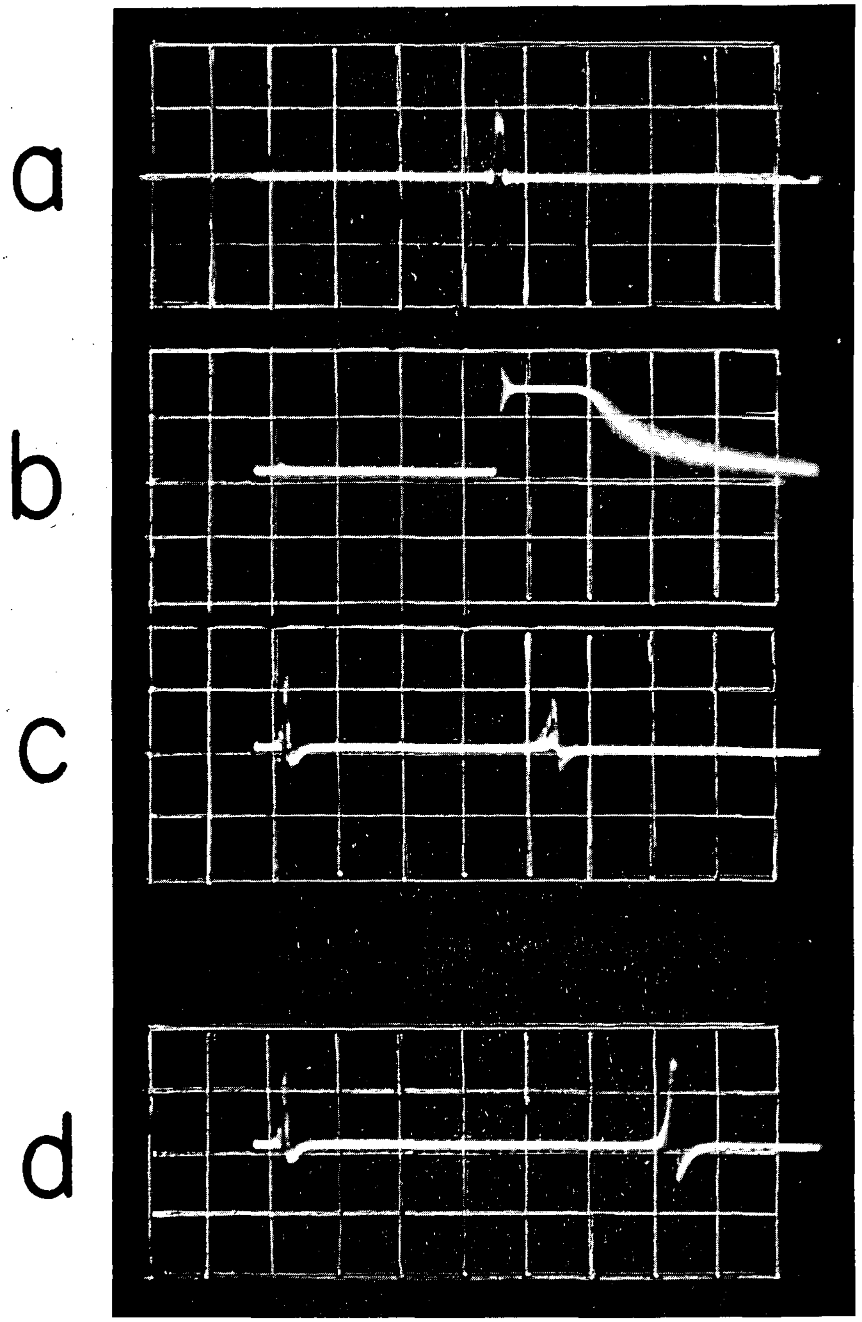

ZN-2394

Fig. 8. (a) Linac beam current to probe at output of linac; (b) Photomultiplier signal with linac beam on, showing blocking of monitor; (c) Photomultiplier signal from 100-kv injector at end of betatron acceleration; (d) Same as (c) with "boosters" on. (Center of scope 100 μsec after trigger. Scope grid: 1-cm squares, 20 μsec/cm.)

## V. FUTURE TESTS

The following plans are an indication of what we would have tried next if the experiments had been continued. No clear-cut plan leading up to accepted beam can be offered, as the course followed would depend on the results obtained by further tests.

First, another photomultiplier and crystal should be made to fit in a different location out of the primary radiation from the linac beam. This would permit observation of spiraling-in of the beam.

Second, a pickup probe or photomultiplier should be mounted on or near the back of the inflector to see if the beam is striking the inflector. To determine how many revolutions are made before striking the inflector requires a resolution of 0.02 μsec per turn. These two experiments should provide the following information: where the beam is going and its lifetime in orbit. No further plans can be presented until the above information is known.

The stray-pickup problems on probes in the synchrotron are fairly difficult. It is expected that even under optimum conditions the maximum beam captured and accelerated would only be comparable to our present beam level. In view of these points and the fact that the machine was to be shut down as soon as possible, no request was made for sufficient time to complete the above tests.

## ACKNOWLEDGMENT

This work was performed under the auspices of the U. S. Atomic Energy Commission.

## APPENDIX

### A. Beam Trajectory in Nonuniform Field

We can determine the displacement and direction of a charged particle moving through a nonuniform magnetic field by the following method. At any point P in the field, the particle has a given radius of curvature $\rho$. Consider a distance near this point such that the change in magnetic field is small and $\rho$ can be considered constant. In going from $P_1$ to $P_2$, an angle $\theta_1$ is swept out and the beam is displaced a distance $d_1$ (see Fig. 9). Similarly, in going from $P_2$ to $P_3$ with a different radius of curvature, angle $\theta_2$ is swept out and the beam is displaced an additional distance $d_2$. The total displacement is then equal to $d_1 + d_2$. This process can be continued to secure the following expression for the total displacement:

$$d_T = \sum_{i=1}^{n} d_i. \tag{1}$$

The beam is deflected through a total angle given by:

$$\phi = \sum_{i=1}^{n} \theta_i. \tag{2}$$

We now wish to evaluate $\theta_i$ and $d_i$ in terms of the radius of curvature $\rho$. If the total angle of deflection is small ($< 15^\circ$) and we take arc lengths $\overline{P_i P_{i+1}}$ equal to unity, we can write $\theta_i = 1/\rho_i$. Therefore, we have from Eq. (2):

$$\phi = \sum_{i=1}^{n} 1/\rho_i. \tag{3}$$

From Fig. 9 we have

$$\text{Sin}\ \alpha_i = d_i/1 = d_i \tag{4}$$

for the chord approximately equal to the arc length. To evaluate $\alpha_i$ we proceed as follows:

$$\alpha_1 = 1/2\ \theta_1$$

$$\alpha_2 = \theta_1 + 1/2\ \theta_2$$

$$\alpha_n = \sum_{i=1}^{n-1} \theta_i + 1/2\ \theta_n.$$

Substituting for $\theta_i$, we have

$$\alpha_n = \sum_{i=1}^{n-1} \frac{1}{\rho_i} + \frac{1}{2\rho_n}.$$

As $\alpha_n$ is less than 15 deg for our case, $\sin \alpha_n \approx \alpha_n$.

Therefore from Eq. (3) we get

$$d_n = \sum_{i=1}^{n-1} \frac{1}{\rho_i} + \frac{1}{2\rho_n} . \qquad (5)$$

The values from Eqs. (3) and (5) are listed for the Berkeley synchrotron in Table I.

## B. Beam Trajectories in the Inflector

By choice, the path through the inflector is circular. We wish to compute the necessary electric field for this path. The force F on a particle of velocity v moving in a magnetic field of strength B is given by e v B, where e is the electronic charge. In an electric field (E), the force F is eE. Therefore, we can equate forces ($eE = e v B$) to find the equivilant electric field. For the case of a relativistic particle the velocity v is approximately the velocity of light (c). This gives $E \approx c B$. Evaluating this we find E/B = 300 volt/cm/gauss.

Using this value for E/gauss, we can change the $H\rho$ values from the charts or graphs to an $E\rho$ value. We can now determine the necessary value of E to bend the 2-Mev injected electrons into a radius $\rho$ of the inflector. In addition, we must add the necessary E to counteract the magnetic field at each point on the trajectory. This gives the total electric field that we must have at each point between the inflector plates. This is tabulated in Table II.

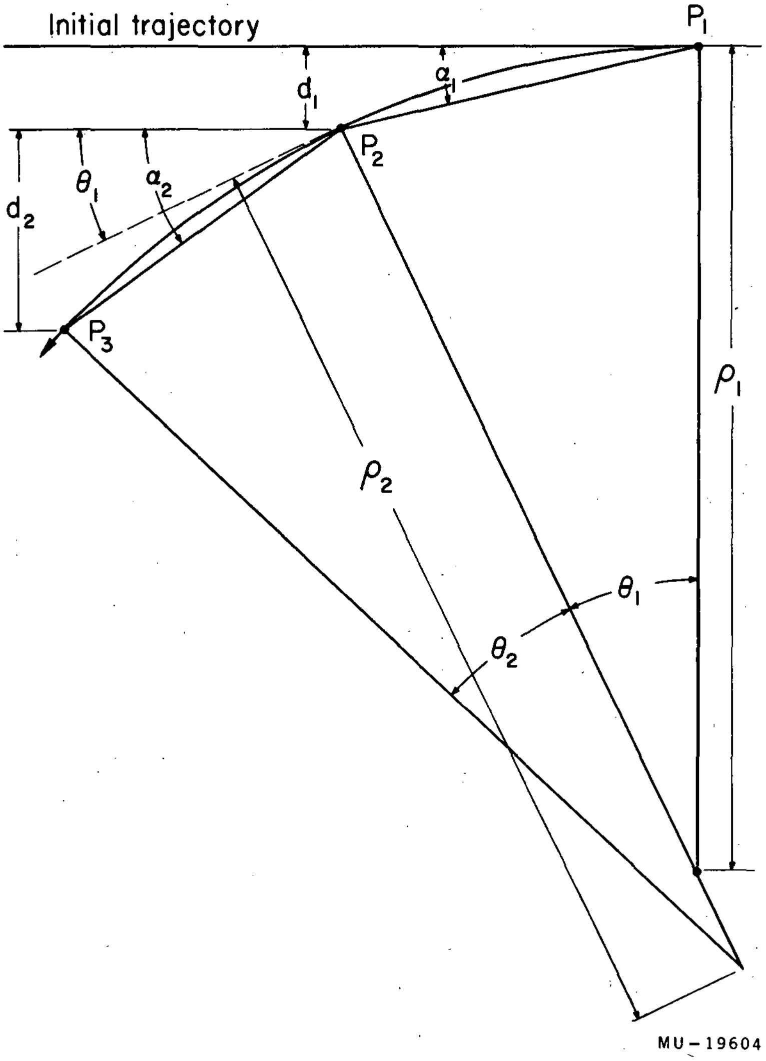

Fig. 9. Geometry for beam-trajectory calculation in nonuniform field.

Table I

Path of particle entering fringe field of synchrotron on target line. Radius of curvature equals 39.4 in. for field of 100 gauss

| Position tangent to orbit at N-S ℄ (in.) | H (%) | $\rho$ (in.) | $1/\rho$ ($\text{in.}^{-1}$) | n | $\phi = \sum_{i=1}^{n} \frac{1}{\rho_i}$ | $d_n$ (in.) | $d_T$ (in.) |
|---|---|---|---|---|---|---|---|
| 41 | 3.7 | 1065 | $0.939 \times 10^{-3}$ | 1 | $0.939\times10^{-3}$ | $0.47\times10^{-3}$ | $0.47\times10^{-3}$ |
| 40 | 4.3 | 916 | 1.09 | 2 | 2.03 | 1.48 | 1.95 |
| 39 | 5.2 | 758 | 1.32 | 3 | 3.35 | 2.69 | 4.64 |
| 38 | 6.0 | 657 | 1.52 | 4 | 4.87 | 4.11 | 8.75 |
| 37 | 7.0 | 563 | 1.78 | 5 | 6.65 | 5.76 | 14.51 |
| 36 | 8.2 | 480 | 2.08 | 6 | 8.73 | 7.69 | 22.20 |
| 35 | 9.2 | 428 | 2.34 | 7 | 11.07 | 9.90 | 32.10 |
| 34 | 10.8 | 365 | 2.74 | 8 | 13.81 | 12.44 | 44.54 |
| 33 | 12.5 | 315 | 3.17 | 9 | 16.98 | 15.40 | 59.94 |
| 32 | 14.0 | 281 | 3.56 | 10 | 20.54 | 18.76 | 78.70 |
| 31 | 16.0 | 246 | 4.06 | 11 | 24.60 | 22.57 | 101.3 |
| 30 | 18.0 | 219 | 4.56 | 12 | 29.16 | 26.88 | 128.2 |
| 29 | 20.5 | 192 | 5.21 | 13 | 34.37 | 31.77 | 159.9 |
| 28 | 23.5 | 168 | 5.91 | 14 | 40.28 | 37.32 | 197.3 |
| 27 | 26.5 | 155 | 6.45 | 15 | 46.73 | 43.50 | 240.8 |
| 26 | 30.3 | 130 | 7.69 | 16 | 54.42 | 50.57 | 291.4 |
| 25 | 34.5 | 114 | 8.77 | 17 | 63.19 | 58.81 | 350.2 |
| 24 | 39.5 | 99.8 | 10.02 | 18 | 73.21 | 68.20 | 418.4 |
| 23 | 44.5 | 88.6 | 11.28 | 19 | 84.49 | 78.85 | 497.3 |
| 22 | 50.5 | 78.0 | 12.82 | 20 | 97.31 | 90.90 | 588.2 |
| 21 | 58.5 | 67.4 | 14.84 | 21 | 112.15 | 104.7 | 692.9 |
| 20 | 67.0 | 58.8 | 17.10 | 22 | 129.25 | 120.7 | 813.6 |
| 19 | 78.5 | 50.2 | 19.92 | 23 | 149.17 | 139.2 | 952.8 |
| 18 | 87.0 | 45.3 | 22.08 | 24 | 171.25 | 160.2 | 1113. |
| 17 | 90.0 | 43.8 | 22.8 | 25 | 194.05 | 182.7 | 1296. |
| 16 | 92.0 | 42.8 | 23.4 | 26 | 217.45 | 205.8 | 1402. |
| 15 | 93.5 | 42.1 | 23.8 | 27 | 241.25 | 219.2 | 1621. |
| 14 | 94.75 | 41.6 | 24.0 | 28 | 265.05 | 253.3 | 1874. |
| 13 | 95.75 | 41.1 | 24.3 | 29 | 289.35 | 277.2 | 2151. |
| 12 | 96.5 | 40.8 | 24.5 | 30 | 313.85 | 301.6 | 2453. |

Table II

Electric field necessary for particle to follow required trajectory through inflector

| Station | H (gauss) | $E_H(\frac{kv}{cm})$ | $E_R(\frac{kv}{cm})$ | $E_T(\frac{kv}{cm})$ |
|---|---|---|---|---|
| orbit | 100 | 24.6 | 61.5 | 86.1 |
| 1 | 97.2 | 23.9 | 61.5 | 85.4 |
| 2 | 97.2 | 23.9 | 61.5 | 85.4 |
| 3 | 96.7 | 23.8 | 61.5 | 85.3 |
| 4 | 96.1 | 23.6 | 61.5 | 85.1 |
| 5 | 95.5 | 23.5 | 61.5 | 85.0 |
| 6 | 94.4 | 23.2 | 61.5 | 84.7 |
| 7 | 92.5 | 22.8 | 61.5 | 84.3 |
| 8 | 89.5 | 22.0 | 61.5 | 83.5 |
| 9 | 83.5 | 20.5 | 61.5 | 82.0 |
| 10 | 65 | 16.0 | 61.5 | 77.5 |
| 10a | 59 | 14.5 | 61.5 | 64.9 |
| 11 | 54 | 13.3 | 61.5 | 66.1 |
| 12 | 45 | 11.1 | 61.5 | 68.3 |
| 13 | 38.5 | 9.47 | 61.5 | 69.9 |

$E_H$ — Electric field to overcome magnetic field.

$E_R$ — Electric field to bend particle in necessary radius ($\rho$).

$E_T$ — Total electric field $E_T = E_H + E_R$.

Stations shown in Fig. 7.

For 2-Mev electrons $E\rho = 2.46 \times 10^3$ (kv/cm)cm.